

PAPER • OPEN ACCESS

Increased flux pinning force and critical current density in MgB_2 by nano- La_2O_3 doping

To cite this article: Danlu Zhang *et al* 2020 *IOP Conf. Ser.: Mater. Sci. Eng.* **756** 012019

View the [article online](#) for updates and enhancements.

You may also like

- [Study on \$\text{La}_2\text{O}_3\$ Wet Clean by pH Controlled Functional Water](#)
Yuichi Ogawa, Iino Hideaki, Fukui Takeo et al.
- [Infrared transmission of \$\text{Na}^+\$ -doped - \$\text{La}_2\text{S}_3\$ ceramics densified by hot pressing](#)
Peisen Li, Wanqi Jie and Huanyong Li
- [Dispersion Effect of \$\text{LaPO}_4\$ Particles in Lithium Ion Conductor LATP](#)
Shigeomi Takai, Masayoshi Uematsu, Wen-Jauh Chen et al.



ECS
The
Electrochemical
Society
Advancing solid state &
electrochemical science & technology

DISCOVER
how sustainability
intersects with
electrochemistry & solid
state science research

Increased flux pinning force and critical current density in MgB₂ by nano-La₂O₃ doping

Danlu Zhang¹, Fang Wan¹, Michael D. Sumption¹, Edward W. Collings¹, CJ Thong², Matt Rindfleisch², Mike Tomsic²

¹ CSMM, Materials Science and Engineering, The Ohio State University, Columbus, OH 43220, USA.

² Hyper Tech Research Inc., Columbus, OH 43228, USA.

zhang.5952@osu.edu

Abstract. MgB₂ superconducting wires and bulks with nano-La₂O₃ addition have been studied. A series of MgB₂ superconducting bulk samples with nano-La₂O₃ addition levels of 0, 5, 7, 18wt% were prepared. AC resistivity data showed slight increases of BC_2 and unchanged B_{irr} for the bulk samples with doping levels lower than 7 wt% and decreased critical fields for the heavily doped (18 wt%) bulk. X-ray diffraction (XRD) showed the presence of LaB₆ in the nano-La₂O₃ doped MgB₂ bulk samples and decreased MgB₂ grain size in nano-La₂O₃ doped bulks. Monocore powder-in-tube (PIT) MgB₂ wires without and with 5 wt% nano-La₂O₃ addition (P-05) were prepared for transport property measurement. 2mol%C-doped *Specialty Materials Inc.* (SMI) boron powder was used for wire P-05 and previously prepared control wires (control wires were made without the addition of nano-La₂O₃ powder, W-00 and P2). Low field magnetic properties were obtained from magnetization loop (M–H), transport critical current density (J_c) was measured at 4.2 K for the nano-La₂O₃ doped PIT wire (P-05) and the control samples (P2 and W-00). The transport critical current density J_c (B) of P-05 at 4.2 K and 8 T (6.0×10^4 A/cm²) was twice that of the control wire. The critical magnetic fields (BC_2 and B_{irr}) of P-05 and the control sample P2 were compared. The critical fields of P-05 were slightly less than those of P2. Kramer-Dew-Hughes plots indicated a change from surface pinning to a mixture of volume pinning and surface pinning. It is shown that enhancement of P-05's transport properties is due to additional flux pinning by the fine-size rare-earth borides rather than enhanced BC_2 or B_{irr} .

1. Introduction

Since the discovery of MgB₂ superconductors in 2001 [1], substantial improvement on the material has been achieved in terms of critical field, transport property, wire manufacture processes. Due to the relatively high T_c (39 K) in MgB₂ and the shortage of liquid helium worldwide, MgB₂ is particularly useful for helium-free MgB₂ MRI magnets [2] and is expected to replace Nb-based MRI magnets in the future. To reach these goals, improvements in the critical current density (J_c) of MgB₂ conductors are necessary.

Numerous approaches have been taken to produce MgB₂ materials with high transport properties: (1) chemical doping of MgB₂ wires [3-5]; (2) cold pressing [6-7]; (3) hot isostatic pressing (HIP) [8-9]; (4) the introduction of the internal magnesium diffusion (IMD) method to address porosity and connectivity issues [10-12]. So far, the best “non-barrier” transport J_c values were obtained by the advanced internal



magnesium infiltration (AIMI) approach, with the addition of C and Dy₂O₃ (1.07×10^5 A/cm²) at 10 T, 4.2 K, [13]. The AIMI technique has the benefit of forming dense MgB₂ layers with improved longitudinal connectivity compared to the extrinsic conventional powder-in-tube (PIT) method, which usually produces wires with randomly connected MgB₂ fibers. On the other hand, the PIT method is favored as a simple and inexpensive approach to studying wire properties in response to chemical doping.

Many chemicals have been added to MgB₂ in the past 18 years to study their effects on the resultant transport and other superconducting properties, such as upper critical field (B_{c2}) [14-15], and irreversibility field (B_{irr}) [16-17]. Generally, improvements in J_c have been attributed to the improvements of either B_{c2} or B_{irr} . Till now, C has been shown to be the most effective doping element for the enhancement of B_{c2} [18] in MgB₂ materials. Many MgB₂ wires with high transport properties were doped with C or C-containing materials. In addition to C and C containing materials, doping with Dy₂O₃ has shown to increase both J_c and B_{irr} [19-20]. In particular, Chen *et al.* [19] and Li *et al.* [20] both demonstrated the effectiveness of a combination of flux pinning by Dy₂O₃ and carrier scattering by C. The effects on the transport J_c of rare earth oxide additions such as Pr₆O₁₁ [21-22], CeO₂ [23], Eu₂O₃ [24] have also been studied.

This paper describes the effect of adding nano-La₂O₃ dopants on superconducting and structural properties in MgB₂ superconductors. La₂O₃ was chosen because some rare-earth oxide additions have improved J_c and B_{c2}/B_{irr} [19-24] in MgB₂ superconductors. Besides, La₂O₃ doping has been previously studied for MgB₂ tapes and nano LaB₆ flux pinning centers as well as increase of J_c in the doped tapes were observed. Therefore, the effects of La₂O₃ doping in MgB₂ wires and bulks were studied here to fully explore the doping effect as well as the optimum doping level. Consequently, four different doping levels (0, 5, 7, 18 wt%) were chosen for the bulks and 5 wt% was chosen to make PIT wires based on the property measured for bulks with the same doping level. Transport J_c in the 5 wt% nano-La₂O₃ doped monocoire PIT-processed MgB₂ wire increased to twice the value of the control sample at 4.2 K, 8 T.

2. Experimental

2.1. Sample preparation

2.1.1. Bulk samples. Four bulk samples B-00 (0 wt% La₂O₃ added), B-05 (5 wt% La₂O₃ added), B-07 (7 wt% La₂O₃ added) and B-18 (18 wt% La₂O₃ added) were made. The precursor powders used were 2 mol% C doped SMI boron powder, Mg powder (325 mesh) from Alfa Aesar, and nano-level (10-100 nm) La₂O₃ powder manufactured by US Research Nanomaterials Inc. The mole ratio of Mg to B powder used was 1: 2. The powder was mixed inside a glove box, and then transferred to a hydraulic press for densification at 5000 psi (or 34.5 MPa). The resulting pellets were heat treated at 850 °C for 30 minutes in flowing Ar, followed by furnace cooling.

2.1.2. Wire Samples. The wire samples were prepared by Hyper Tech Research using their well-known “continuous tube filling and forming” (CFTT) powder-in-tube (PIT) process [25] followed by wire drawing to 0.83 mm in diameter. Selected for controls were two samples from previous studies. Designated P2 [26] and W-00 [27] precursor powders were 2 mol% C doped B from SMI and Mg powder as in the undoped bulk. The sample specifications are listed in Table 1.

Table 1. Info on bulk and PIT wire samples

Sample Form	Sample Name	Wt% La ₂ O ₃	Heat Treatment	Crystallite size (nm)
Bulk	B-00	0	30min/850°C	20.6
Bulk	B-05	5	30min/850°C	19.8
Bulk	B-07	7	30min/850°C	7.6
Bulk	B-18	18	30min/850°C	17

Wire	P2*	0	20min/675°C	-
Wire	W-00*	0	60min/650°C	-
Wire	P-05	5	60min/650°C	-

*Previously made/published [26][27]
Both referred to as “Control”

2.2. Measurements

2.2.1. X-Ray diffraction (XRD) measurement. The powdered bulk samples were scanned on a Rigaku Miniflex 600 XRD machine at a scan rate of 5 deg / min. Phases and peaks were studied with the help of PDXL software.

2.2.2. AC resistivity. The AC resistivity vs temperature measurements on the bulk samples were performed on a Quantum Design Model 6000 Physical Property Measuring System (PPMS). The bulk samples were cut into rectangular prisms and four-point probe measurements were used to obtain sample resistance of 5 K to 45 K. The usual “10% normal resistivity” and “90% normal resistivity” rules were used to obtain B_{irr} and B_{c2} , respectively.

2.2.3. Transport J_c measurement. The transport J_c measurements were carried out in transverse magnetic fields of up to 12 T in a liquid He bath at 4.2 K on samples 50 mm long with a gauge length of 5 mm and an electric field criterion of 1 μ V/cm. Measurements were also done using a gauge length of 4 mm. The layer J_c of the CTFF PIT strands were calculated using the critical transport currents divided by the MgB₂ layer area.

2.2.4. Magnetic J_c measurement. Magnetization-Magnetic field (M-H) loops were measured under VSM mode in a Quantum Design Model 6000 Physical Property Measuring System (PPMS) on sample P-05 3.2 mm long. Magnetic J_{cm} at 4.2 K was extracted from M-H loop at a ramp rate of 10 mT/s in transverse fields of up to 9 T. Based on Bean’s model [28], the 4.2 K magnetic J_{cm} for the superconducting CTFF monocoil strand and was derived from:

$$J_{cm} = \frac{3 \cdot \pi \cdot \Delta M}{4 \cdot d},$$

where d is the diameter of the MgB₂ layer inside the wire and ΔM is the full height of the M-H loop at a certain field. The magnetic J_{cm} played a role in the pinning force calculation (see section 3.4).

3. Results and Discussion

3.1. Bulk sample’s magnetic and structure properties

B_{c2} and B_{irr} values were obtained for MgB₂ bulks doped with nano-La₂O₃ and the control bulk sample (B-00) at temperatures of 16 K ~ 36 K, Figure 1. B_{irr} stayed unchanged for B-05 and B-07. B_{c2} increased by 0.2 T with the addition of 5 wt% La₂O₃ and increased by 0.4 T with addition of 7 wt% La₂O₃. However, both B_{c2} and B_{irr} decreased significantly in response to doping with 18 wt% La₂O₃. Based on the data in Figure 1, it can be seen that T_c of the doped bulks did not change compared to the control bulk sample. This is similar to the unchanged T_c observation on Dy₂O₃ doped MgB₂ bulks [29], meaning no significant atomic substitution occurred on MgB₂ host lattice sites.

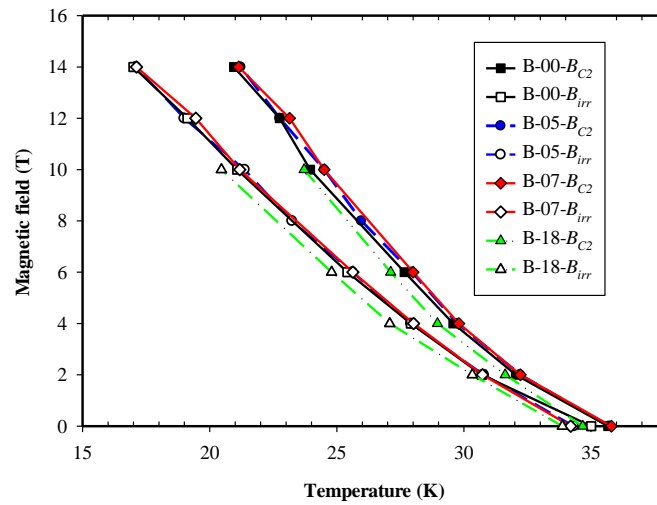


Figure 1. Critical magnetic fields as a function of temperatures for undoped bulk sample (B-00) and doped samples (B-05, B-07, B-18).

Phases and peaks in the MgB_2 bulk samples have been studied with the aid of XRD. The patterns shown in Figure 2 indicates the presence of LaB_6 in all doped bulk samples (shown by green arrows), presumably there are pinning centers. The MgB_2 peaks of B-05 and B-07, which is consistent with the minor increases of B_{c2} seen in Figure 1. The lattice shifts are smaller than those observed by Gao *et al.* [30] in MgB_2 tapes with acetone and La_2O_3 additions. Usually MgB_2 peak shifts observed in XRD patterns are caused by atomic substitution and/or strain. The shifts seen in Figure 3 is probably due to the lattice strain generated by the nanoparticles (such as LaB_6) since T_c was shown to be unchanged in doped samples. MgB_2 grain size was estimated based on XRD data using William-Hall method, Table 1. As the La_2O_3 doping level increases from 0 wt% to 7 wt%, MgB_2 grain size decreased from 20.6 nm to 7.6 nm. The grain size of MgB_2 was 17 nm in the heavily doped sample. Yuan [27] observed same trend in his Dy_2O_3 doped MgB_2 bulks [27]. He attributed this grain size reduction to secondary phase DyB_6 nanoparticles. Here, the reduction of grain size in La_2O_3 doped MgB_2 bulks might be due to the secondary phase LaB_6 , which inhibits the grain growth and pins fluxons.

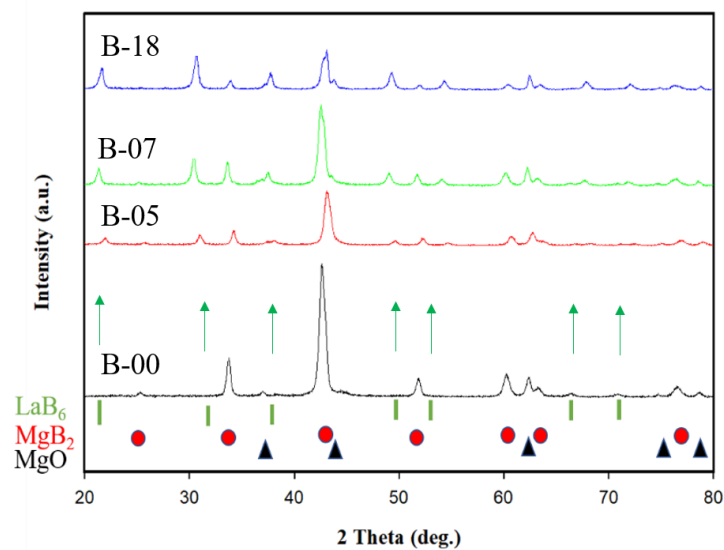


Figure 2. XRD patterns for undoped MgB₂ bulk and MgB₂ bulks doped with nano-La₂O₃.

3.2. Wire strength, transport and magnetic properties

This paper also describes the effect of 5 wt% nano-La₂O₃ addition to MgB₂ PIT wires. Two previously-made control samples (P2 [26] and W-00 [27]) were used for reference. These two wires were interchangeably used not only because the compositions are the same and the heat treatment procedures are very similar, but also because measured data from two controls combined can offer complete data for comparison purpose in this paper. Though they were manufactured from different batches, these mono PIT wires (with the use of 2mol%C-doped B powder) usually possess consistent properties. The transport properties of PIT MgB₂ wire P-05 and undoped wires P2 and W-00 were measured at 4.2 K in transverse magnetic fields up to 12 T, Figure 3. It can be seen that La₂O₃ doping resulted in a significant increase in J_c . In particular, at 8 T and 4.2 K, the J_c of P-05 is 6.0×10^4 A/cm², about twice that of the control wire P2. It is important to keep in mind that AIMI approach usually produces MgB₂ wires with higher J_c compared to conventional PIT method for wires with same composition and heat treatment procedure because of the enhanced connectivity. Thus, AIMI-produced wires are not discussed here.

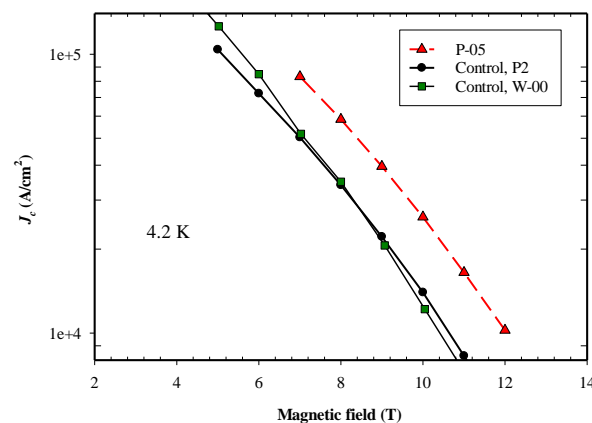


Figure 3. Critical current density (J_c) as a function of magnetic field for control wire and the La₂O₃ doped sample P-05 at 4.2 K.

3.3. Wire sample: Critical fields and flux pinning

In order to enquire into the factors responsible for the enhancement of J_c , the critical fields (B_{c2} and B_{irr}) were measured via resistivity approach in the PPMS in Figure 4. The T_c of P-05 decreased with the addition of La₂O₃ and its B_{c2} decreased by about 1 T at lower temperatures and very insignificantly at higher temperatures. Likewise, its B_{irr} decreased by around 0.6 T at lower temperatures and by a smaller amount at higher temperatures. A decrease in the Kramer field, B_k (a surrogate for B_{irr}) of 1.0 T at 4.2 K (Figure 5) confirms the above result. The relatively larger B_{c2} values in the undoped wires could be due to the existence of nano-level electron scattering centers (e.g., grain boundaries, point defects, volume defects and secondary phases). Since these two wires shown on Figure 4 are manufactured at different heat treatment conditions, it is very likely that fine secondary impurity phases such as MgO, B₂O₃ were introduced in the undoped wire P2 and therefore enhanced B_{c2} to a slight degree.

Two common mechanisms for enhancing J_c in MgB₂ wires are to enhance B_{irr} or enhance B_{c2} . Here, we propose another mechanism for enhanced J_c in MgB₂ wires with nano-La₂O₃ doping. It is well known that enhanced transport J_c by way of C doping in MgB₂ wire can be attributed to enhanced B_{c2} by way of enhanced scattering effect [16, 19]. The increased transport J_c in Dy₂O₃-doped MgB₂ wire was

attributed to an increase in B_{irr} [19-20]. With regard to La_2O_3 doped wire samples, as mentioned above, the 4.2 K, 8 T, J_c of P-05 was about twice that of the undoped control wire. But this increase is accompanied by no changes or decreases in B_{c2} and B_{irr} (1 T and 0.6 T, respectively, at lower temperatures), Figure 4. Clearly, a mechanism other than critical field is responsible for the increase in J_c ; flux pinning is the obvious choice.

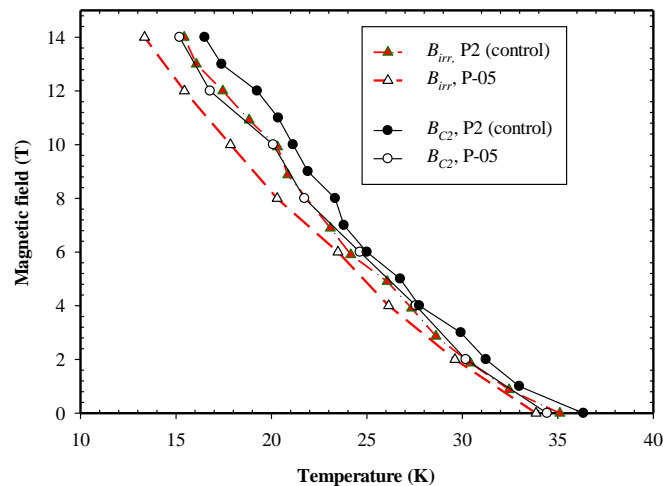


Figure 4. Upper critical field and irreversibility field for the control sample and nano- La_2O_3 added PIT MgB_2 wire P-05.

To further study the phenomena, Kramer plot has been made, A Kramer Plot, $J_c^{0.5}B^{0.25}$ vs. B , was shown in Figure 5. The irreversibility fields based on Kramer model [31], B_k , was taken at the x-axis intercepts of linear fittings (evenly spaced dashed lines) on Figure 5. B_k of the doped wire has a lower value than the control wire value, which agrees with the critical field analysis done above on the wire samples.

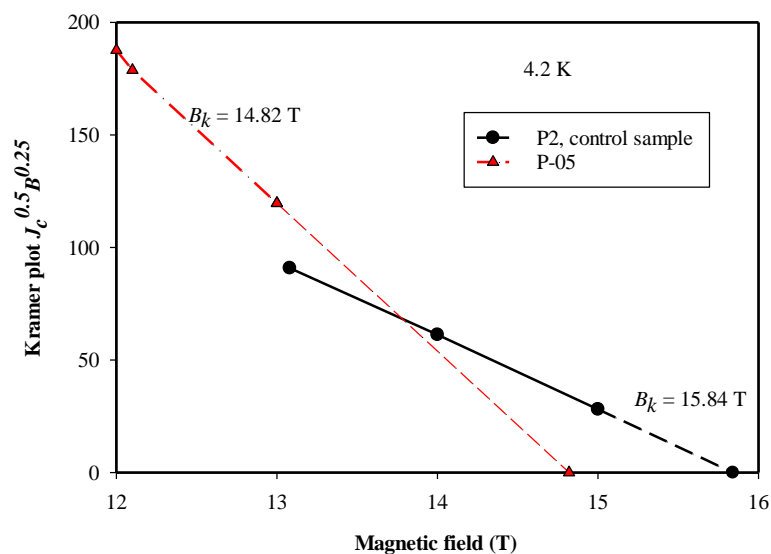


Figure 5. Kramer plot ($J_c^{0.5}B^{0.25}$ vs. B) for control wire sample and P-05 at 4.2 K. The irreversibility fields based on the Kramer model [31], B_k , were taken as the extrapolated x-axis intercepts of linear fittings (evenly spaced dashed lines).

3.4. Flux pinning in response to La_2O_3 doping

Using data derived from the M-H loop, the normalized flux pinning force density $F_p/F_{p,max}$ was plotted against normalized magnetic field $b=B/B_k$ at 20 K to avoid flux jump effect, Figure 6(a). B_k here was derived based on magnetic measurement conducted at 20 K in PPMS. Figure 6(b) showed the J_c data measured by transport and magnetic methods. Apparently, magnetic measured J_c agrees well with the transport data for P-05. Based on Dew-Hughes's analysis [32] about $f_p \propto b^{1/2}(1-b)^2$, the curve for the control sample which peaks at $B/B_k=0.2$ is indicative of grain boundary pinning. In contrast, the curve for P-05 wire peaked at around $b=0.168$. This phenomenon has been observed in Dy_2O_3 doped samples [29] and Yang *et al.* [29] stated that two reasons can be responsible for this behaviour: (1) The doped sample might contain a set of local B_k s instead of one distinct value, which can lead to an artificial error in the estimation of the peak positions; (2) The deviation from $b_{peak}=0.2$ might be due to other pinning mechanisms (e.g., normal volume pinning in which f_p maximizes at $b < 0.2$ due to anisotropy [33]) in association with the GB pinning. The presence of LaB_6 peaks in all the XRD patterns of the doped bulk samples strongly suggests that LaB_6 , formed by reaction with the B powder, would also be present in the doped wires and as such would be responsible for the observed volume pinning.

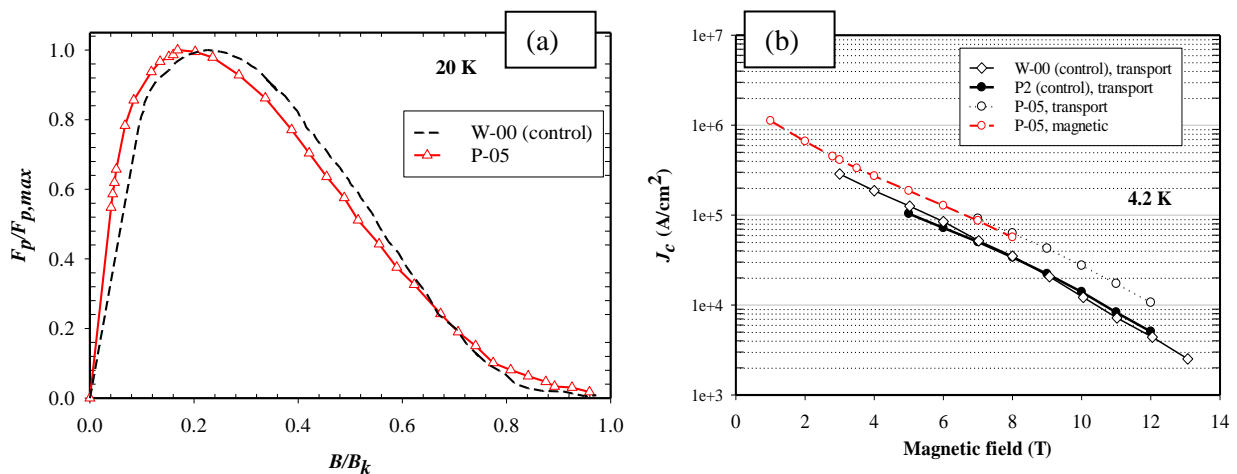


Figure 6. (a, left) Normalized flux pinning force as a function of reduced field for control sample and the doped wire, P05, based on the magnetic data; (b, right) Critical current density measured for wire P-05 using both magnetic measurement and transport measurement.

4. Concluding Discussion

Four MgB_2 bulk samples with 0-18 wt% nano- La_2O_3 additions and a monocoil PIT MgB_2 wire with 5 wt% nano- La_2O_3 addition were prepared for measurements of J_c , B_{irr} , BC_2 and magnetic and transport J_c (see Table 1). Resistive measurements of B_{irr} and BC_2 in response to La_2O_3 doping were made in the PPMS on the bulk and wire samples. For the bulks B_{irr} remained unchanged in B-05 and B-07 but decreased in B-18; BC_2 increased by 0.2 T in B-05 and 0.4 T in B-07 but also decreased in B-18. For the wires (controls and P-05) B_{irr} decreased by ~ 0.6 T at low temperatures and a smaller amount at high temperatures. BC_2 decreased by 1 T at low temperatures (resistive results and Kramer plot) and insignificantly at high temperatures. The 4.2 K, 8 T, J_c of P-05 was about twice that of the undoped control. There is no correlation between changes in the critical fields and J_c . On the other hand, the occurrence of LaB_6 in the XRD patterns and the shapes of the normalized flux pinning curves (after Dew-Hughes) indicate that the increase in J_c is a consequence of increased flux pinning in the doped wire.

5. References

- [1] Nagamatsu J, Nakagawa N, Muranaka T, Zenitani Y and Akimitsu J 2001 *Nature* **410** 63
- [2] Zhang D, Kovacs C, Rochester J, Majoros M, Wan F, Sumption M D, Collings E W, Rindfleisch M, Panik D, Doll D and Avonce R 2018 *Supercond. Sci. Technol.* **31** 085013
- [3] Matsumoto A, Kumakura H, Kitaguchi H and Hatakeyama H 2003 *Supercond. Sci. Technol.* **16** 926
- [4] Ma Y, Zhang X, Xu A, Li X, Xiao L, Nishijima G, Awaji S, Watanabe K, Jiao Y, Xiao L and Bai X 2005 *Supercond. Sci. Technol.* **19** 133
- [5] Woźniak M, Hopkins S C, Gajda D and Glowacki B A 2012 *Phys. Procedia* **36** 1594-8
- [6] Hossain M S, Senatore C, Flükiger R, Rindfleisch M A, Tomsic M J, Kim J H and Dou S X 2009 *Supercond. Sci. Technol.* **22** 095004
- [7] Wan F, Sumption M D, Rindfleisch M A and Collings E W 2017 *IOP Conference Series: Materials Science and Engineering* Vol. **279**, No. 1, p. 012024
- [8] Gajda D, Morawski A, Zaleski A, Cetner T, Malecka M, Presz A, Rindfleisch M, Tomsic M, Thong C J and Surdacki P 2013 *Supercond. Sci. Technol.* **26** 115002
- [9] Prikhna T, Gawalek W, Savchuk Y, Soldatov A, Sokolovsky V, Eisterer M, Weber H W, Noudem Serga M, Turkevich V and Tomsic M 2011 *J SUPERCOND NOV MAGN* **24** 137-50
- [10] Li G Z, Sumption M D, Zwayer J B, Susner M A, Rindfleisch M A, Thong C J, Tomsic M J and Collings E W 2013 *Supercond. Sci. Technol.* **26** 095007
- [11] Ye S J, Matsumoto A, Togano K and Kumakura H 2011 *Physica C* **471** 1133-6
- [12] Kováč P, Hušek I, Melišek T, Kopera L and Kulich M 2016 *Supercond. Sci. Technol.* **29** 10LT01
- [13] Li G Z, Sumption M D, Susner M A, Yang Y, Reddy K M, Rindfleisch M A, Tomsic M J, Thong C J and Collings E W 2012 *Supercond. Sci. Technol.* **25** 115023
- [14] Patnaik S, Gurevich A, Bu S D, Kaushik S D, Choi J, Eom C B, Larbalestier D C 2004 *Phys. Rev. B* **70** 064503
- [15] Angst M, Bud'ko S L, Wilke R H and Canfield P C 2005 *Phys. Rev. B* **71** 144512
- [16] Sumption M D, Bhatia M, Dou S X, Rindfleisch M, Tomsic M, Arda L, Ozdemir M, Hascicek Y and Collings E W 2004 *Supercond. Sci. Technol.* **17** 1180
- [17] Wang J, Bugoslavsky Y, Berenov A, Cowey L, Caplin A D, Cohen L F, MacManus Driscoll J L, Cooley L D, Song X and Larbalestier D C 2002 *Appl. Phys. Lett.* **81** 2026-8
- [18] Dai W, Ferrando V, Pogrebnjakov A V, Wilke R H, Chen K, Weng X, Redwing J, Bark C W, Eom C B, Zhu Y and Voyles P M 2011 *Supercond. Sci. Technol.* **24** 125014
- [19] Chen S K, Wei M, MacManus-Driscoll J L 2006 *Appl. Phys. Lett.* **88** 192512
- [20] Li G Z, Sumption M D, Rindfleisch M A, Thong C J, Tomsic M J and Collings E W 2014 *Appl. Phys. Lett.* **105** 112603
- [21] Pan X F, Shen T M, Li G, Cheng C H and Zhao Y 2007 *Phys. Status Solidi A*. **204** 1555-60
- [22] Ojha N, Malik VK, Bernhard C and Varma G D 2010 *Phys. Status Solidi A*. **207** 175-82
- [23] Pan X F, Cheng C H and Zhao Y 2011 *J SUPERCOND NOV MAGN* **24** 1611-6
- [24] Ojha N, Malik V K, Bernhard C and Varma G D 2009 *Physica C* **469** 846-51
- [25] Tomsic M, Rindfleisch M, Yue J, McFadden K, Doll D, Phillips J, Sumption M D, Bhatia M, Bohnenstiehl S and Collings E W 2007 *Physica C* **456** 203-8
- [26] Li G Z, Yang Y, Susner M A, Sumption M D, Collings E W 2011 *Supercond. Sci. Technol.* **25** 025001
- [27] Yang Y 2016 Influence of Chemical Doping on Microstructures and Superconducting Properties of MgB₂ Wires and Bulk Samples (Doctoral dissertation, The Ohio State University)
- [28] Sumption M D, Peng X, Lee E, Wu X and Collings E W 2004 *Cryogenics* **44** 711
- [29] Yang Y, Sumption M D and Collings E W 2016 *Sci. Rep.* **6** 29306
- [30] Gao Z, Wei Y M, Wang D, Z Xian-Ping, Satoshi A and Kazuo W 2010 *Chin. Phys. Lett.* **27** 117401
- [31] E. J. Kramer 1973 *J. Appl. Phys.* **44** 1360
- [32] Dew-Hughes D 1974 *Phil. Mag.* **30** 293-305
- [33] Eisterer M 2008 *Phys. Rev. B*. **77** 144524